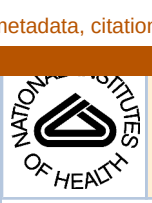

Published in final edited form as:

Mol Ther. 2008 September ; 16(9): 1624–1629. doi:10.1038/mt.2008.120.

Sustained Dystrophin Expression Induced by Peptide-conjugated Morpholino Oligomers in the Muscles of *mdx* Mice

Natee Jearawiriyapaisarn[1,2], **Hong M Moulton**[3], **Brian Buckley**[3], **Jennifer Roberts**[1], **Peter Sazani**[3], **Suthat Fucharoen**[1,2], **Patrick L Iversen**[3], and **Ryszard Kole**[1,3]

[1]*Department of Pharmacology and Lineberger Comprehensive Cancer Center, University of North Carolina at Chapel Hill, Chapel Hill, North Carolina, USA* [2]*Thalassemia Research Center and Institute of Molecular Biology and Genetics, Mahidol University, Bangkok, Thailand* [3]*AVI BioPharma, Inc., Corvallis, Oregon, USA*

Abstract

Cell-penetrating peptides (CPPs), containing arginine (R), 6-aminohexanoic acid (X), and/or β-alanine (B) conjugated to phosphorodiamidate morpholino oligomers (PMOs), enhance their delivery in cell culture. In this study, the potency, functional biodistribution, and toxicity of these conjugates were evaluated *in vivo*, in EGFP-654 transgenic mice that ubiquitously express the aberrantly spliced EGFP-654 pre-mRNA reporter. Correct splicing and enhanced green fluorescence protein (EGFP) upregulation serve as a positive readout for peptide-PMO (PPMO) entry into cells and access to EGFP-654 pre-mRNA in the nucleus. Intraperitoneal injections of a series of PPMOs, A-N (12 mg/kg), administered once a day for four successive days resulted in splicing correction in numerous tissues. PPMO-B was highly potent in the heart, diaphragm, and quadriceps, which are key muscles in the treatment of Duchenne muscular dystrophy. We therefore investigated PPMO M23D-B, designed to force skipping of stop-codon containing dystrophin exon 23, in an *mdx* mouse model of the disease. Systemic delivery of M23D-B yielded persistent exon 23 skipping, yielding high and sustained dystrophin protein expression in body-wide muscles, including cardiac muscle, without detectable toxicity. The rescued dystrophin reduced serum creatinine kinase to near-wild-type levels, indicating improvement in muscle integrity. This is the first report of oligonucleotide-mediated exon skipping and dystrophin protein induction in the heart of treated animals.

Introduction

In order to enhance the efficacy of antisense oligonucleotides as therapeutic agents, numerous chemical modifications have been introduced to their bases, backbones, and internucleotide linkages.[1] One such modification, phosphorodiamidate morpholino oligomers (PMOs),[2,3] bind their RNA targets with high affinity and specificity, and are highly resistant to nucleolytic degradation; however, their systemic distribution and functionality were found to be modest in mouse model systems.[4] Subsequently, conjugates of PMOs with arginine-rich cell-penetrating peptides (CPPs), termed peptide-PMOs (PPMOs), were found to possess enhanced potency *in vitro*.[5–8] In particular, serum and intracellular stability of peptides was increased, endosomal trapping was reduced, and nuclear uptake was enhanced by the introduction of non-α amino acids, namely, 6-aminohexanoic acid (X) and β-alanine (B), into the oligoarginine (R_8) peptides.[9–12]

Correspondence: Ryszard Kole, AVI BioPharma, Inc., Corvallis, Oregon, USA. E-mail: E-mail: kole@aribio.com.

In this study, a series of PPMOs carrying CPPs consisting of R_8 residues and a variable number of X and/or B residues (termed A through N, Table 1) was designed. The series was first evaluated in EGFP-654 transgenic mice, which ubiquitously express an enhanced green fluorescence protein (EGFP) pre-mRNA interrupted by an aberrantly spliced human β-globin IVS2-654 intron. The EGFP upregulation serves as a positive readout for the ability of PPMOs to enter cells and correct aberrant splicing of the EGFP-654 pre-mRNA in the nucleus[4] (Figure 1a). After delivery through intraperitoneal (IP) injection, all PPMOs exhibited a broad tissue distribution and corrected the aberrant splicing in EGFP-654 mice to varying degrees.

One of the conjugates, PPMO-B, was very effective in the heart, diaphragm, and quadriceps, the target muscles for treatment of Duchenne muscular dystrophy (DMD), a severe progressive muscle wasting disorder.[13] This work focused on the use of PPMO-B in the treatment of DMD in an *mdx* mouse model of the disease. We found that systemic delivery of a PPMO-B targeted to exon 23 of the dystrophin gene (M23D-B) induced high and sustained dystrophin protein expression in body-wide muscles in treated *mdx* mice. This led to improved cardiac histology and a dramatic drop in serum creatinine kinase (CK), a hallmark of improvement in muscle integrity.

Results

Functional biodistribution of PPMO-654 conjugates in EGFP-654 mice

In order to evaluate the *in vivo* potency and functional biodistribution of PPMOs, EGFP-654 mice were injected IP once a day for 4 days at 12 mg/kg/day with PPMO-654 conjugates (A through N, Table 1), targeted to the aberrant 5′-splice site in EGFP-654 pre-mRNA (Figure 1a). One day after the last injection, the mice were killed, and total RNA was isolated from tissues and analyzed using reverse transcriptase-PCR (RT-PCR). The results show that all the PPMO-654 conjugates exhibited broad tissue-wide distribution, with significant splicing correction in most tissues (Figure 1b) (but not in brain and bone marrow; Supplementary Figure 1a), which was substantially higher than that achieved with higher doses of unconjugated PMOs.[4]

The number and position of 6-aminohexanoic acid (X) and/or β-alanine (B) residues inserted in the oligoarginine (R_8) in the CPPs significantly affected the potency and functional biodistribution of the PPMOs. PPMO-A, containing 8 arginines, 1 X residue and 1 B residue was very effective in modifying EGFP-654 pre-mRNA splicing in liver (~63%), but was much less effective in several other tissues including the quadriceps and the heart (Figure 1b). In contrast, PPMO-B was the most effective in the quadriceps (100%) and the heart (59%), but its efficacy in the liver was similar to that of PPMO-A. PPMO-J was highly effective in the kidney (100%) and quadriceps (100%) but not in the heart (21%). Surprisingly, all the PPMOs corrected the EGFP-654 splicing in diaphragm 100%. Overall, the differences in the functional biodistribution of PMOs conjugated with a family of closely related peptides are striking, and more structure-activity studies are needed to elucidate the causes and mechanisms of these differences.

We noticed that PPMO-B is the most potent in all muscle tissues, especially the heart. PPMO-B did not produce toxicity in mice at the doses tested (Figure 1c and Supplementary Figure 1b), and the data in Figure 2a and b show a clear dose–response in the heart and quadriceps, while in the diaphragm, even at the low dose of 3 mg/kg, 100% of correctly spliced EGFP mRNA was produced. Therefore, PPMO-B represents a promising candidate for the treatment of DMD. The strategy developed in our laboratory[14,15] is to induce in-frame skipping of an offending exon which causes a premature termination codon, restoring production of functional dystrophin protein (Supplementary Figure 2).

In order to determine the persistence of PPMO-B activity, EGFP-654 mice were injected intravenously (IV) at 12 mg/kg/day for 4 days, and killed up to 12 weeks after the last injection (Figure 2c); IV administration of PPMO-B was more efficient than IP and subcutaneous routes, especially in the heart (Supplementary Figure 3). The splicing correction in the heart reached 90% at 1 day after the last injection and then gradually decreased, but was still detectable (~10%) at 6 weeks. In the diaphragm, 100% correctly spliced EGFP mRNA was detectable up to 2–3 weeks after the last injection, decreasing to 10–40% at 12 weeks. Impressively, PPMO-B exhibited 100% splicing correction in the quadriceps up to 12 weeks after the last injection.

The expression of EGFP was also followed-up in live animals using the Xenogen IVIS 100 imaging system (Figure 2d). The EGFP signal was detectable in the abdominal fascia and quadriceps from 1 week after the last injection, and increased for up to 5 weeks without any decrease in fluorescence intensity at week 8. A PPMO targeted to mouse dystrophin with three mismatches (PPMO mis-23D), used as a negative control, did not upregulate EGFP.

Skipping of dystrophin exon 23 in *mdx* mice by PPMO M23D-B

The phenotype of the *mdx* mouse is caused by a premature termination codon in exon 23 of the dystrophin gene (Supplementary Figure 2), which prevents translation of dystrophin protein. Oligonucleotide-induced skipping of exon 23 during splicing of dystrophin pre-mRNA restores the reading frame in the spliced mRNA, resulting in the production of partially functional truncated dystrophin protein in the skeletal muscles of *mdx* mice.[16–18] Recently, the systemically delivered unconjugated morpholino oligonucleotide, PMO M23D, targeted to a donor splice site of mouse dystrophin intron 23, was found to be effective in skeletal muscles but, importantly, not in the heart.[19,20] Given that, as described earlier in the text, PPMO-B was highly efficient and persistent in splicing correction in the heart, diaphragm, and quadriceps in EGFP-654 mice, we synthesized the PPMO M23D-B conjugate for treating *mdx* mice.

The *mdx* mice were injected IV once every day for 4 days with M23D-B at 12 mg/kg/day (Figure 3). Muscle tissues were collected and analyzed at the indicated time points for exon skipping, by nested RT-PCR of dystrophin mRNA. In the heart, the exon 23–skipped dystrophin mRNA reached 70% at 1 day after the last injection and decreased to 50 and 20% at 2 and 7 weeks, respectively; at 9 weeks after the last injection, exon 23 skipping was still detectable. In the diaphragm and quadriceps, M23D-B induced almost complete exon 23 skipping, and this remained essentially unchanged up to 9 weeks after the last injection. Similar activity was detected in all the other skeletal muscles (Supplementary Figure 4). No exon 23–skipped transcript was observed in saline or mismatched oligo-treated *mdx* mice or in wild-type C57BL6 mice (data not shown).

Analysis of total protein from M23D-B-treated mice by in-gel immunostaining with anti-dystrophin antibody (Figure 4a) showed that, in the heart, the dystrophin levels reached ~30% of wild-type at 2–3 weeks and remained at ~15% up to 7 weeks after the last injection. This is the first report of oligonucleotide-mediated exon skipping and dystrophin protein induction in the heart. In the diaphragm and quadriceps, significant dystrophin production, 40–50% of wild type, was achieved and maintained for up to 17 weeks after the last injection (Figure 4a). The multiple dystrophin bands detected in samples from wild-type and treated *mdx* mice were naturally occurring variants or synthetic intermediates of dystrophin.[21] These results clearly confirm that the persistent skipping of exon 23 induced by M23D-B resulted in robust translation of dystrophin protein, which persisted for up to 17 weeks after the last injection, and localized correctly at the periphery of muscle fibers (Figure 4b). As expected, no detectable dystrophin protein was observed in untreated *mdx* mice.

The discrepancy between the level of exon skipping in mRNA (100%) and the level of induced dystrophin protein (40–50%) relative to wild type suggests that RT-PCR overestimates the extent of exon-skipped mRNA. This is not surprising, considering that nested PCRs were required. Note, however, that we used a total of 30 cycles in the PCR, which compares favorably with published 55 cycle nested PCR protocols.[18] It is also possible that the full-length dystrophin mRNA carrying premature termination codon in exon 23 may be degraded by nonsense-mediated decay, resulting in overestimation of corrected dystrophin mRNA. Nevertheless, the important observation is that therapeutically relevant levels[22,23] of dystrophin were produced in all key muscle types: skeletal muscle, diaphragm, and heart.

The sera collected during the experiment were tested for CK, a marker for heart and skeletal muscle membrane instability.[24,25] Figure 5a demonstrates a dramatic reduction in the level of serum CK from ~30,000 to <2,000 U/l 1 day after the last injection. Commensurate with additional increases in dystrophin in subsequent weeks (Figure 4a), serum CK levels were further reduced to ~500 U/l. This level was maintained for 11 weeks after the last injection, and increased only at 17 weeks, the time point at which dystrophin protein was barely detectable in the heart, and somewhat decreased in the diaphragm and quadriceps. A similar pattern was observed for circulating levels of aspartate aminotransferase and alanine aminotransferase (Figure 5b), which are present in a variety of extrahepatic tissues, including cardiac and skeletal muscles confirming that the restored dystrophin protein improved the integrity of muscle sarcolemma. Specifically to the heart, cardiac muscle stained with hematoxylin and eosin showed significant reduction of inflammatory cell infiltration in *mdx* mice treated with M23D-B at 3 weeks after the last injection (Figure 5c), suggesting that necrosis in cardiac muscle was significantly reduced.

Discussion

In this study, we first used EGFP-654 mice to evaluate the potential of peptide-conjugated PMOs as splice-switching oligonucleotides. This mouse model provides a positive readout for functional biodistribution data, indicating where the conjugates are functionally active. The results clearly show that systemically delivered PPMOs corrected EGFP-654 splicing to a high degree in a number of different tissues, and were essentially nontoxic at the doses used in the study. Comparison with an unconjugated PMO that was investigated in previous experiments in the same animal model indicates that the CPPs altered the functional biodistribution of PPMOs and significantly enhanced their potency and intracellular delivery.[4] The effects of the CPPs are dependent on the number and position of the non-α amino acids, aminohexanoic acid (X), and/or β-alanine (B) (X and/or B residues). These differences could be attributable to the stability of the conjugates in serum and cells,[11] or to their ability to escape from endosomes/lysosomes.[12]

In EGFP-654 mice, PPMO-B delivered by IV injection at 12 mg/kg/day for 4 days was highly potent in splicing correction in cardiac muscle, diaphragm, and quadriceps, and its activity persisted in these muscles for at least 2–3 months. Therefore, we applied its equivalent, PPMO M23D-B, in the treatment of muscular dystrophy in *mdx* mice. Systemic delivery of M23D-B induced skipping of exon 23, thereby restoring and sustaining dystrophin protein expression which localized correctly at the plasma membrane of muscle fibers in body-wide muscles, including the heart. It is also important to note that the smooth muscles of the digestive tract are impaired in DMD;[26] PPMO-B has an effect on these tissues, *e.g.*, stomach, small intestine, and colon (Supplementary Figure 1a), and should therefore provide amelioration of related symptoms in patients.

Induction of exon 23 skipping mediated by M23D-B conjugate was significantly more efficient than that mediated by the unconjugated PMO.[19] More importantly, the M23D-B showed

induction of exon skipping, production of induced dystrophin protein, and histological improvement in cardiac muscle, the first such results using an antisense oligonucleotide. Given that 30% of deaths in DMD patients are caused by cardiomyopathy,[27] it is crucial to induce dystrophin expression in cardiac muscle. Clearly, the expression of dystrophin ameliorated the sarcolemmal integrity of muscles, leading to dramatic decreases in serum CK, aspartate aminotransferase, and alanine aminotransferase, and reduced the extent of muscle necrosis in the heart.

Materials and Methods

PPMO conjugates

The sequences of CPPs are indicated in Table 1. All PPMOs were synthesized and purified as described by Wu *et al*.[8] and targeted to the aberrant 5′-splice site in the intron of EGFP-654 pre-mRNA. (PPMO-654; 5′-GCT ATT ACC TTA ACC CAG-3′).[4] PPMO M23D-B was targeted to the 5′-splice site of intron 23 (5′-GGC CAA ACC TCG GCT TAC CTG AAA T-3′) of mouse dystrophin pre-mRNA.[28] A mismatched M23D-B (mis-23D-B, 5′-GCG CAA ACC TCG CGT TAC CGT AAA T-3′) was used as a control. In all EGFP-654 PPMOs, the CPPs were conjugated at the 5′-end; in M23D-B, peptide B was conjugated at the 3′-end. All PPMOs were resuspended and diluted in sterile normal saline.

Animal treatment

All experiments involving animals were approved by Institutional Animal Care and Use Committee at the University of North Carolina. PPMOs were delivered once daily to 7–8-week-old EGFP-654 or C57BL/10ScSn^{mdx} (*mdx*; Jackson Laboratory, Bar Harbor, ME) mice by IP, IV, or subcutaneous injections at the indicated doses for 4 days. The mice were killed by CO_2 inhalation, and the tissues were removed and stored at −80 °C for RNA isolation or fixed in 4% paraformaldehyde[4,29] for EGFP visualization. For immunofluorescence, muscle tissues from *mdx* mice were mounted in Tissue-Tek optimal cutting temperature embedding medium (Sakura, Torrance CA), snap-frozen in isopentane, and stored at –80 °C.

RNA isolation and analysis

Total RNA was isolated from ~1–5 mg tissue with TRI Reagent (Molecular Research Center, Cincinnati, OH) as per the manufacturer's protocol. The EGFP mRNA was amplified by RT-PCR as described earlier,[29] except that 1 μl of 0.1 mmol/l of Cy5-deoxycytidine triphosphate (GE Healthcare, Amersham, UK) was added into the PCR instead of ^{32}P-labeled deoxyadenosine triphosphate. The dystrophin mRNA was amplified using nested RT-PCR. Total RNA (400 ng) was subjected to RT-PCR (5′-GTT CAG CTT CAC TCT TTA TCT TCT GCC-3′, reverse outer primer; 5′-CAA TGT TTC TGG ATG CAG ACT TTG TGG-3′, forward outer primer) with rTth DNA polymerase (Applied Biosystems, Foster City, CA). Reverse transcription was at 70 °C for 15 minutes; PCR was at 95 °C for 3 minutes, followed by 8 cycles of 95 °C for 1 minute, 55 °C for 1 minute, and 72 °C for 1 minute. One microliter of the reaction was then subjected to nested PCR with Platinum *Taq* DNA polymerase (Invitrogen, Carlsbad, CA) and labeled with Cy5-deoxycytidine triphosphate (forward inner primer 5′-CAC ATC TTT GAT GGT GTG AGG-3′; reverse inner primer 5′-CAA CTT CAG CCA TCC ATT TCT G-3′). The nested PCR was carried out for 22 cycles as described earlier. The RT-PCR products from EGFP and dystrophin mRNAs were separated on 10% nondenaturing polyacrylamide gels (Invitrogen) and scanned on Typhoon 9400 Imager (GE Healthcare, Amersham, UK). The ImageQuant TL (version 2005) analysis software was used for quantifying the intensity of bands.

Protein extraction and in-gel immunodetection

Total protein was extracted from muscle samples using the total protein extraction kit (Millipore, Billerica, MA) as per the manufacturer's protocol, and quantified using the Quick Start Bradford protein assay kit (Bio-Rad Laboratories, Hercules, CA). Total protein (100 μg) was loaded onto NuPAGE 3–8% Tris-acetate gels and electrophoresed in 1× NuPAGE Tris–acetate–SDS running buffer (Invitrogen, Carlsbad, CA). Dystrophin was visualized by in-gel immunodetection. After electrophoresis, the gel was fixed in 50% isopropanol/5% acetic acid for 15 minutes, washed in water for 15 minutes, and incubated overnight at room temperature with NCL-DYS2, a mouse monoclonal antibody against C-terminus of dystrophin (Novocastra, Newcastle upon Tyne, UK), diluted in StartingBlock (phosphate-buffered saline) blocking buffer (1:50; Pierce, Rockford, IL). The gel was then washed in PBST (phosphate-buffered saline and 0.1% Tween-20) three times for 10 minutes each, and incubated for 2 hours at room temperature with the IRDye 680 goat anti-mouse IgG (LI-COR, Lincoln, NE) secondary antibody, diluted in StartingBlock (phosphate-buffered saline) blocking buffer (1:1,000). After three 20-minute washes in PBST and in phosphate-buffered saline overnight, the gel was scanned and quantitated using Odyssey infrared imaging system (LI-COR).

Dystrophin immunofluorescence and muscle histology

The 8-μm muscle sections were examined for dystrophin expression using NCL-DYS2 mouse monoclonal antibody and an M.O.M. kit (Vector Laboratories, Burlingame, CA). Briefly, the sections were incubated with primary antibody at a dilution of 1:20 for 2 hours at room temperature, followed by incubation with the biotinylated anti-mouse IgG for 1 hour and fluorescein avidin D cell sorting for 5 minutes. Mounted sections were visualized using a Zeiss Axio microscope at ×100 magnification. Sections were stained with hematoxylin and eosin for histological analysis, carried out by Animal Histopathology Core Facility (Lineberger Comprehensive Cancer Center, University of North Carolina, Chapel Hill, NC).

Live animal fluorescence imaging

In vivo fluorescent imaging was performed using Xenogen IVIS 100 (Caliper Life Sciences, Hopkinton, MA). The mice were anesthetized with 2.5% isoflurane. After hair removal with depilatory lotion, the mice were placed on the warmed camera box with continuous exposure to 2.5% isoflurane. Fluorescent images were acquired and analyzed using Live Image 2.2 software.

Clinical biochemistry

Analyses of serum aspartate aminotransferase, alanine aminotransferase, blood urea nitrogen, creatinine, and CK were performed at the Animal Clinical Laboratory Core Facility (University of North Carolina) using a Vitro 250 Chemical Analyzer (Ortho-Clinical Diagnostics, Rochester, NY).

Supplementary Material

Refer to Web version on PubMed Central for supplementary material.

Acknowledgements

We thank Leshara Fulton for her excellent technical assistance, and Thipparat Suwanmanee and all members of our laboratory for advice and encouragement. N.J. was partially supported by the Royal Golden Jubilee (RGJ) scholarship from the Thailand Research Fund. This work was supported by the National Institutes of Health grant PO1-GM059299 to R.K.

References

1. Kurreck J. Antisense technologies. Improvement through novel chemical modifications. Eur J Biochem 2003;270:1628–1644. [PubMed: 12694176]
2. Summerton J. Morpholino antisense oligomers: the case for an RNase H-independent structural type. Biochim Biophys Acta 1999;1489:141–158. [PubMed: 10807004]
3. Arora V, Devi GR, Iversen PL. Neutrally charged phosphorodiamidate morpholino antisense oligomers: uptake, efficacy and pharmacokinetics. Curr Pharm Biotechnol 2004;5:431–439. [PubMed: 15544491]
4. Sazani P, Gemignani F, Kang SH, Maier MA, Manoharan M, Persmark M, et al. Systemically delivered antisense oligomers upregulate gene expression in mouse tissues. Nat Biotechnol 2002;20:1228–1233. [PubMed: 12426578]
5. Abes R, Arzumanov AA, Moulton HM, Abes S, Ivanova GD, Iversen PL, et al. Cell-penetrating-peptide-based delivery of oligonucleotides: an overview. Biochem Soc Trans 2007;35(Pt 4):775–779. [PubMed: 17635146]
6. Lebleu B, Moulton HM, Abes R, Ivanova GD, Abes S, Stein DA, et al. Cell penetrating peptide conjugates of steric block oligonucleotides. Adv Drug Deliv Rev 2007;60:517–529. [PubMed: 18037527]
7. Abes R, Arzumanov A, Moulton H, Abes S, Ivanova G, Gait MJ, et al. Arginine-rich cell penetrating peptides: design, structure-activity, and applications to alter pre-mRNA splicing by steric-block oligonucleotides. J Pept Sci 2008;14:455–460. [PubMed: 18236382]
8. Wu RP, Youngblood DS, Hassinger JN, Lovejoy CE, Nelson MH, Iversen PL, et al. Cell-penetrating peptides as transporters for morpholino oligomers: effects of amino acid composition on intracellular delivery and cytotoxicity. Nucleic Acids Res 2007;35:5182–5191. [PubMed: 17670797]
9. Moulton HM, Nelson MH, Hatlevig SA, Reddy MT, Iversen PL. Cellular uptake of antisense morpholino oligomers conjugated to arginine-rich peptides. Bioconjug Chem 2004;15:290–299. [PubMed: 15025524]
10. Amantana A, Moulton HM, Cate ML, Reddy MT, Whitehead T, Hassinger JN, et al. Pharmacokinetics, biodistribution, stability and toxicity of a cell-penetrating peptide-morpholino oligomer conjugate. Bioconjug Chem 2007;18:1325–1331. [PubMed: 17583927]
11. Youngblood DS, Hatlevig SA, Hassinger JN, Iversen PL, Moulton HM. Stability of cell-penetrating peptide-morpholino oligomer conjugates in human serum and in cells. Bioconjug Chem 2007;18:50–60. [PubMed: 17226957]
12. Abes S, Moulton HM, Clair P, Prevot P, Youngblood DS, Wu RP, et al. Vectorization of morpholino oligomers by the (R-Ahx-R)4 peptide allows efficient splicing correction in the absence of endosomolytic agents. J Control Release 2006;116:304–313. [PubMed: 17097177]
13. Lovering RM, Porter NC, Bloch RJ. The muscular dystrophies: from genes to therapies. Phys Ther 2005;85:1372–1388. [PubMed: 16305275]
14. Sierakowska H, Sambade MJ, Agrawal S, Kole R. Repair of thalassemic human β-globin mRNA in mammalian cells by antisense oligonucleotides. Proc Natl Acad Sci USA 1996;93:12840–12844. [PubMed: 8917506]
15. Wilton SD, Lloyd F, Carville K, Fletcher S, Honeyman K, Agrawal S, et al. Specific removal of the nonsense mutation from the mdx dystrophin mRNA using antisense oligonucleotides. Neuromuscul Disord 1999;9:330–338. [PubMed: 10407856]
16. Mann CJ, Honeyman K, Cheng AJ, Ly T, Lloyd F, Fletcher S, et al. Antisense-induced exon skipping and synthesis of dystrophin in the mdx mouse. Proc Natl Acad Sci USA 2001;98:42–47. [PubMed: 11120883]
17. Lu QL, Mann CJ, Lou F, Bou-Gharios G, Morris GE, Xue SA, et al. Functional amounts of dystrophin produced by skipping the mutated exon in the mdx dystrophic mouse. Nat Med 2003;9:1009–1014. [PubMed: 12847521]
18. Lu QL, Rabinowitz A, Chen YC, Yokota T, Yin H, Alter J, et al. Systemic delivery of antisense oligoribonucleotide restores dystrophin expression in body-wide skeletal muscles. Proc Natl Acad Sci USA 2005;102:198–203. [PubMed: 15608067]

19. Alter J, Lou F, Rabinowitz A, Yin H, Rosenfeld J, Wilton SD, et al. Systemic delivery of morpholino oligonucleotide restores dystrophin expression bodywide and improves dystrophic pathology. Nat Med 2006;12:175–177. [PubMed: 16444267]

20. Fletcher S, Honeyman K, Fall AM, Harding PL, Johnsen RD, Wilton SD. Dystrophin expression in the mdx mouse after localised and systemic administration of a morpholino antisense oligonucleotide. J Gene Med 2006;8:207–216. [PubMed: 16285002]

21. Nicholson LV, Davison K, Falkous G, Harwood C, O'Donnell E, Slater CR, et al. Dystrophin in skeletal muscle. I. Western blot analysis using a monoclonal antibody. J Neurol Sci 1989;94:125–136. [PubMed: 2693617]

22. Wells DJ, Wells KE, Asante EA, Turner G, Sunada Y, Campbell KP, et al. Expression of human full-length and minidystrophin in transgenic mdx mice: implications for gene therapy of Duchenne muscular dystrophy. Hum Mol Genet 1995;4:1245–1250. [PubMed: 7581360]

23. Phelps SF, Hauser MA, Cole NM, Rafael JA, Hinkle RT, Faulkner JA, et al. Expression of full-length and truncated dystrophin mini-genes in transgenic mdx mice. Hum Mol Genet 1995;4:1251–1258. [PubMed: 7581361]

24. Glesby MJ, Rosenmann E, Nylen EG, Wrogemann K. Serum CK, calcium, magnesium, and oxidative phosphorylation in mdx mouse muscular dystrophy. Muscle Nerve 1988;11:852–856. [PubMed: 3173410]

25. McArdle A, Edwards RH, Jackson MJ. How does dystrophin deficiency lead to muscle degeneration? —evidence from the mdx mouse. Neuromuscul Disord 1995;5:445–456. [PubMed: 8580726]

26. Barohn RJ, Levine EJ, Olson JO, Mendell JR. Gastric hypomotility in Duchenne's muscular dystrophy. N Engl J Med 1988;319:15–18. [PubMed: 3380114]

27. Foster K, Foster H, Dickson JG. Gene therapy progress and prospects: Duchenne muscular dystrophy. Gene Ther 2006;13:1677–1685. [PubMed: 17066097]

28. Gebski BL, Mann CJ, Fletcher S, Wilton SD. Morpholino antisense oligonucleotide induced dystrophin exon 23 skipping in mdx mouse muscle. Hum Mol Genet 2003;12:1801–1811. [PubMed: 12874101]

29. Roberts J, Palma E, Sazani P, Ørum H, Cho M, Kole R. Efficient and persistent splice switching by systemically delivered LNA oligonucleotides in mice. Mol Ther 2006;14:471–475. [PubMed: 16854630]

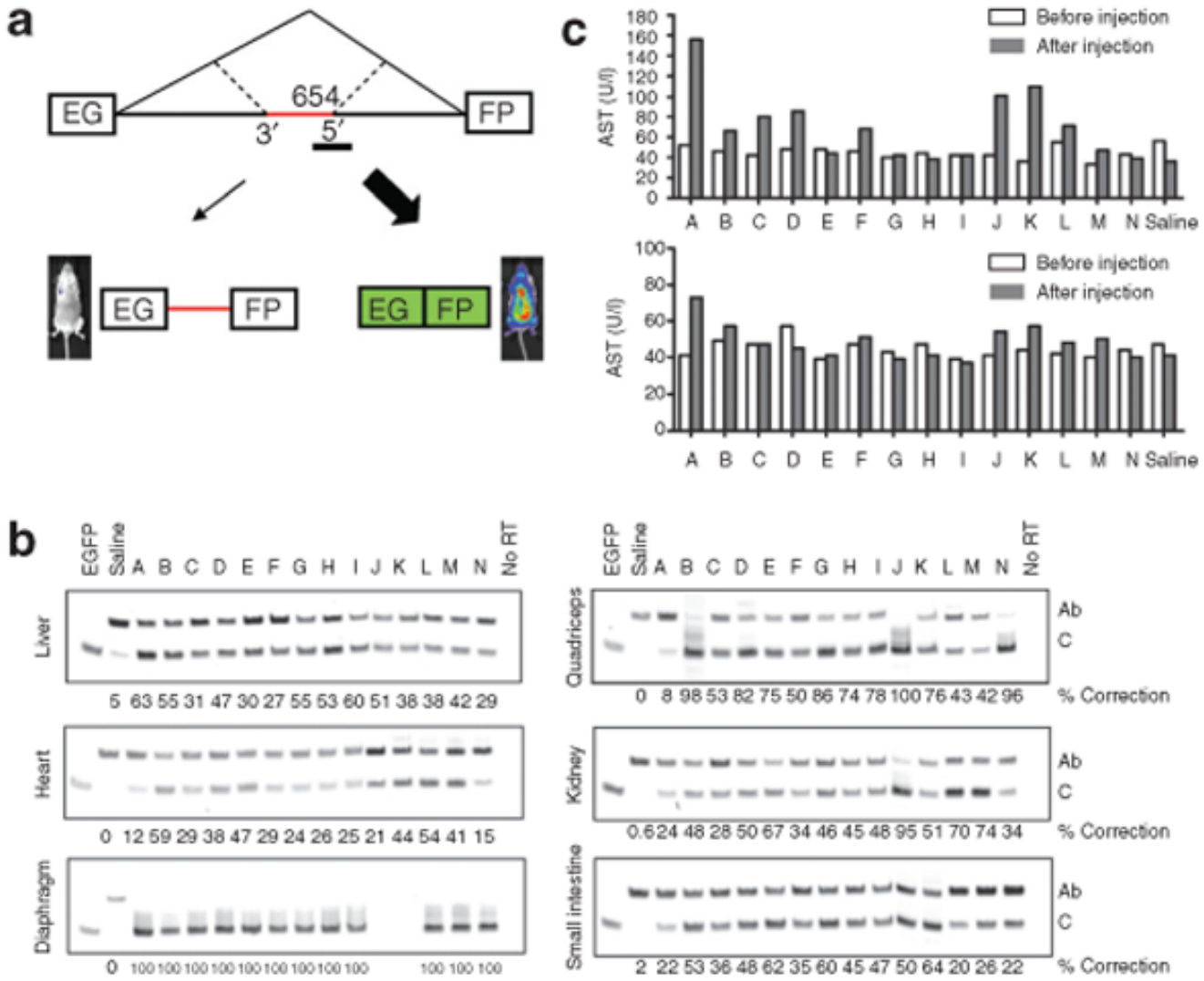

Figure 1. Correction of aberrant splicing in EGFP-654 mice by PPMO-654 conjugates, and the toxicity of the conjugates

(**a**) The EGFP-654 mice express a modified EGFP-654 pre-mRNA in which the enhanced green fluorescence protein (EGFP) coding region (boxes) is interrupted by an aberrantly spliced human β-globin IVS2-654 intron (line). The aberrantly spliced mRNA retains an intron fragment (red line), preventing proper translation of EGFP. Blocking the aberrant 5′-splice site with PPMO-654 (shaded bar) restores the correct splicing, leading to EGFP upregulation. The EGFP upregulation in mice is observed using a fluorescent live imaging system. (**b**) Reverse transcriptase-PCR (RT-PCR) of total RNA from the tissues of PPMO-treated EGFP-654 mice. The EGFP-654 mice were treated with PPMO-654 conjugates by intraperitoneal injection once every day for 4 days at 12 mg/kg/day. RNA samples were extracted from the indicated tissues of the treated mice and analyzed using RT-PCR 1 day after the last injection. The Cy5-labeled RT-PCR products from aberrantly spliced and correctly spliced EGFP mRNA are shown as Ab [160 base pairs (bp)] and C (87 bp), respectively. (**c**) Levels of serum aspartate aminotransferase and alanine aminotransferase were monitored before the treatment and at 1 day after the last injection of PPMO-654 conjugates. PPMO, peptide-phosphorodiamidate morpholino oligomer.

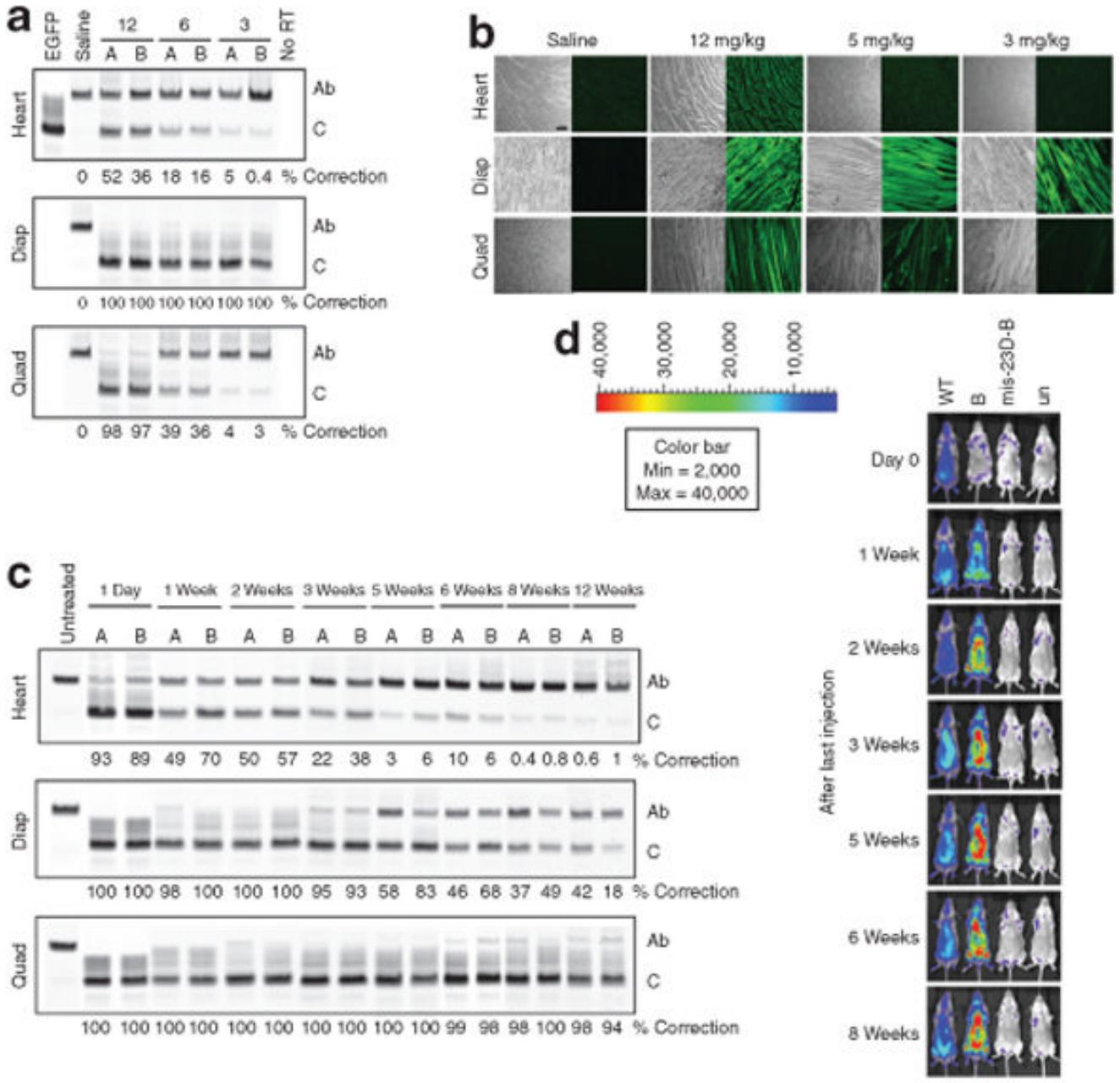

Figure 2. Effective and persistent splicing correction of PPMO-B conjugate in the heart, diaphragm (diap), and quadriceps (quad) of EGFP-654 mice

(**a–b**) Dose-dependent splicing correction. EGFP-654 mice were treated with PPMO-B conjugate at the indicated doses by intravenous (IV) injection once every day for 4 days. (**a**) Reverse transcriptase-PCR (RT-PCR) of total RNA and (**b**) fluorescent images of tissue sections were analyzed 1 day after the last injection. Samples A and B are from different mice. (Scale bar = 100 μm). (**c–d**) Time-dependent splicing correction. The EGFP-654 mice were injected IV with PPMO-B conjugate at 12 mg/kg/day for 4 days. (**c**) Total RNA samples from the heart, diap, and quad were analyzed using RT-PCR at the indicated time points. (**d**) Upregulation of enhanced green fluorescence protein (EGFP) expression was monitored using a fluorescent live imaging system. WT is a mouse that constitutively expresses EGFP. The

EGFP-654 mice treated with PPMO-B, the control mice treated with PPMO-B at 12 mg/kg, and untreated mice are shown as B, scr-B, and un, respectively. PPMO, peptide-phosphorodiamidate morpholino oligomer.

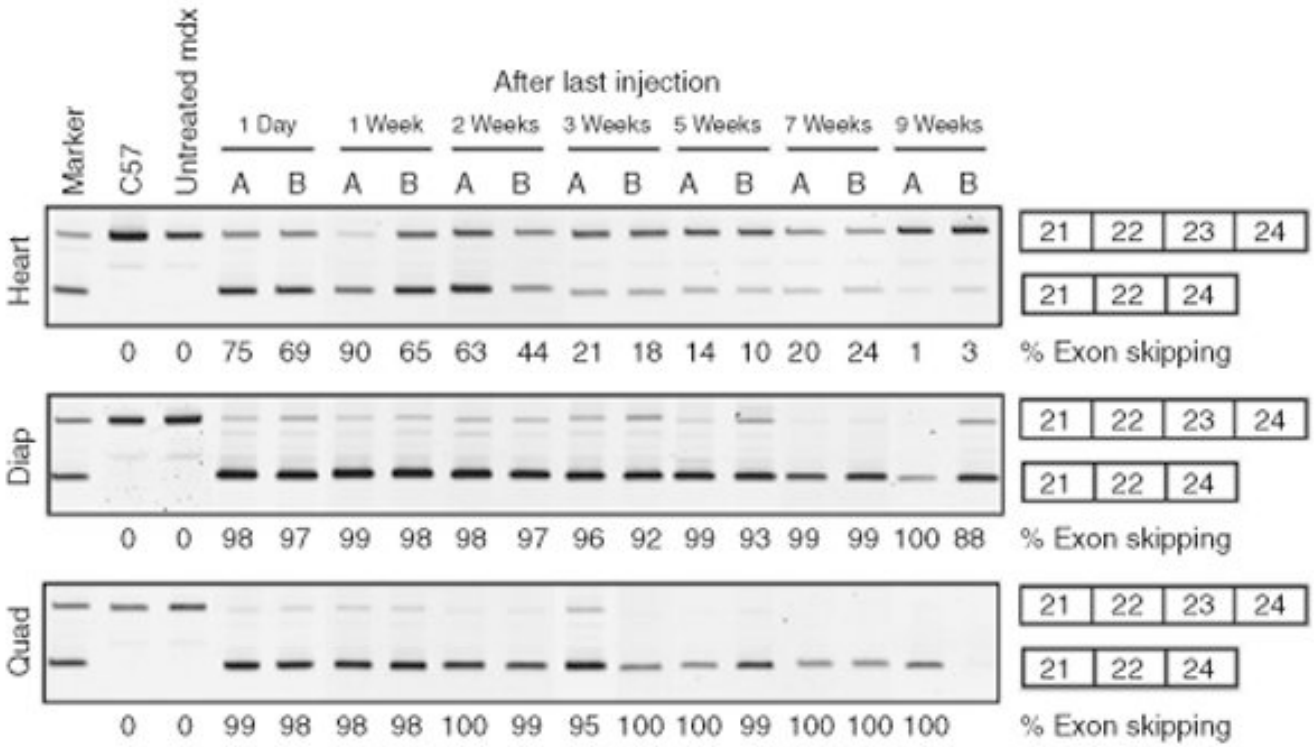

Figure 3. Persistence of M23D-B-induced exon 23 skipping of dystrophin transcript in the heart, diaphragm (diap), and quadriceps (quad) of *mdx* mice after intravenous injection at 12 mg/kg/day for 4 days

RNA samples were analyzed using nested reverse transcriptase-PCR (RT-PCR) at the indicated time points. The nested RT-PCR product from the full-length dystrophin transcript is 445 base pairs (bp), indicated by boxes numbered 21–24. The product from exon 23–skipped mRNA is 232 bp, as indicated by boxes numbered 21, 22, and 24.

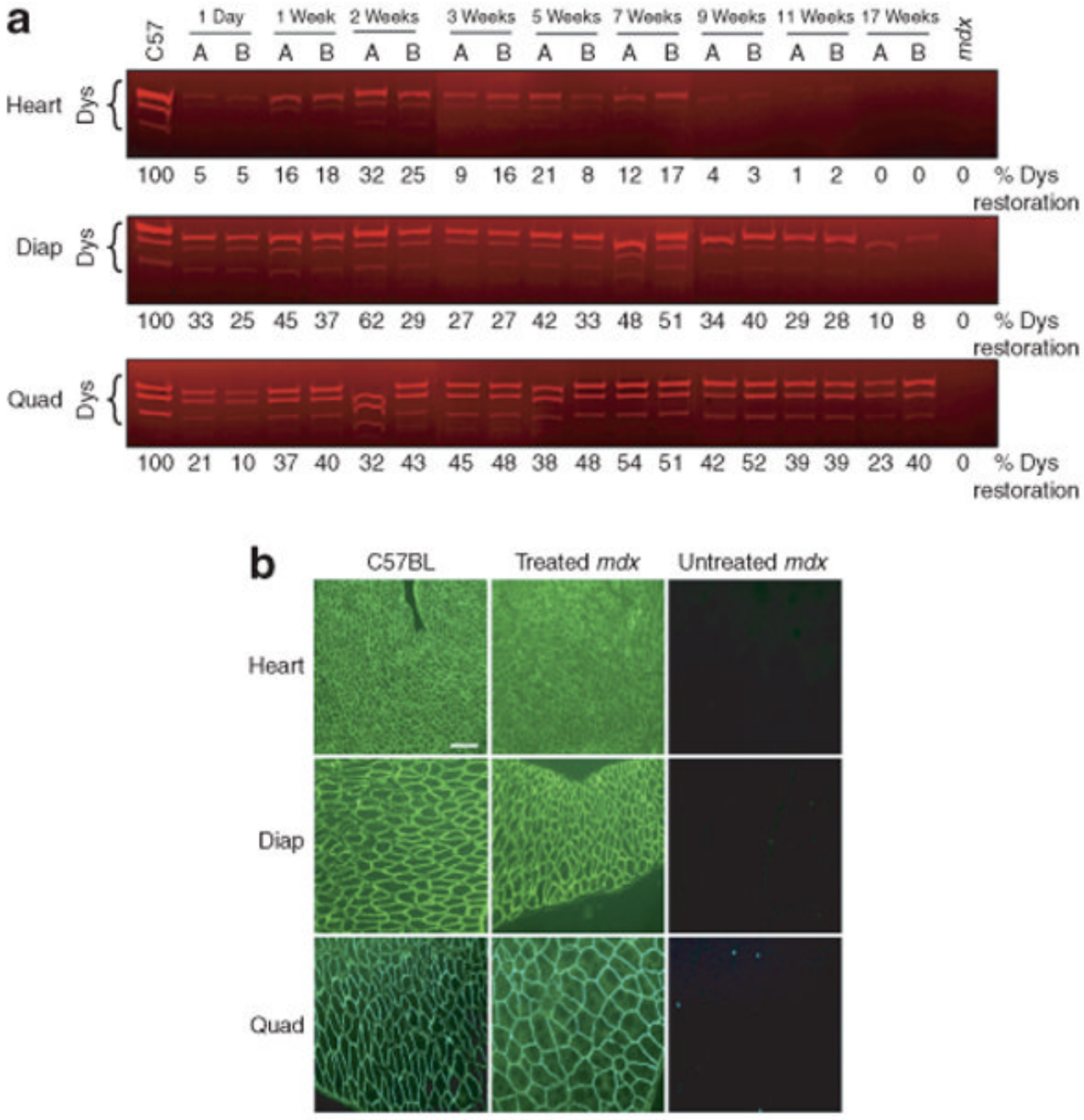

Figure 4. Restoration of dystrophin (Dys) expression in the heart, diaphragm (diap), and quadriceps (quad) of M23D-B-treated mice after intravenous injections at 12 mg/kg/day for 4 days

(**a**) In-gel western blot detection of total protein extracted from injected *mdx* muscles at the indicated time points. Dys protein was detected by mouse monoclonal antibody against C-terminus of Dys, followed by IRDye 680 goat anti-mouse immunoglobulin G (IgG) antibody. The three different Dys bands represent naturally occurring variants or synthetic intermediates of Dys. (**b**) Immunofluorescence detection of Dys on frozen muscle sections from the heart, diap, and quad of treated *mdx* mice. Sections were immunostained for Dys with NCL-DYS2 and detected using biotinylated anti-mouse IgG and fluorescein avidin. Sections from the heart, diap, and quad were analyzed 3, 2, and 2 weeks after the last injection, respectively. Muscle

sections from C57BL and untreated *mdx* mice were included as positive and negative controls, respectively. Scale bar, 100 μm.

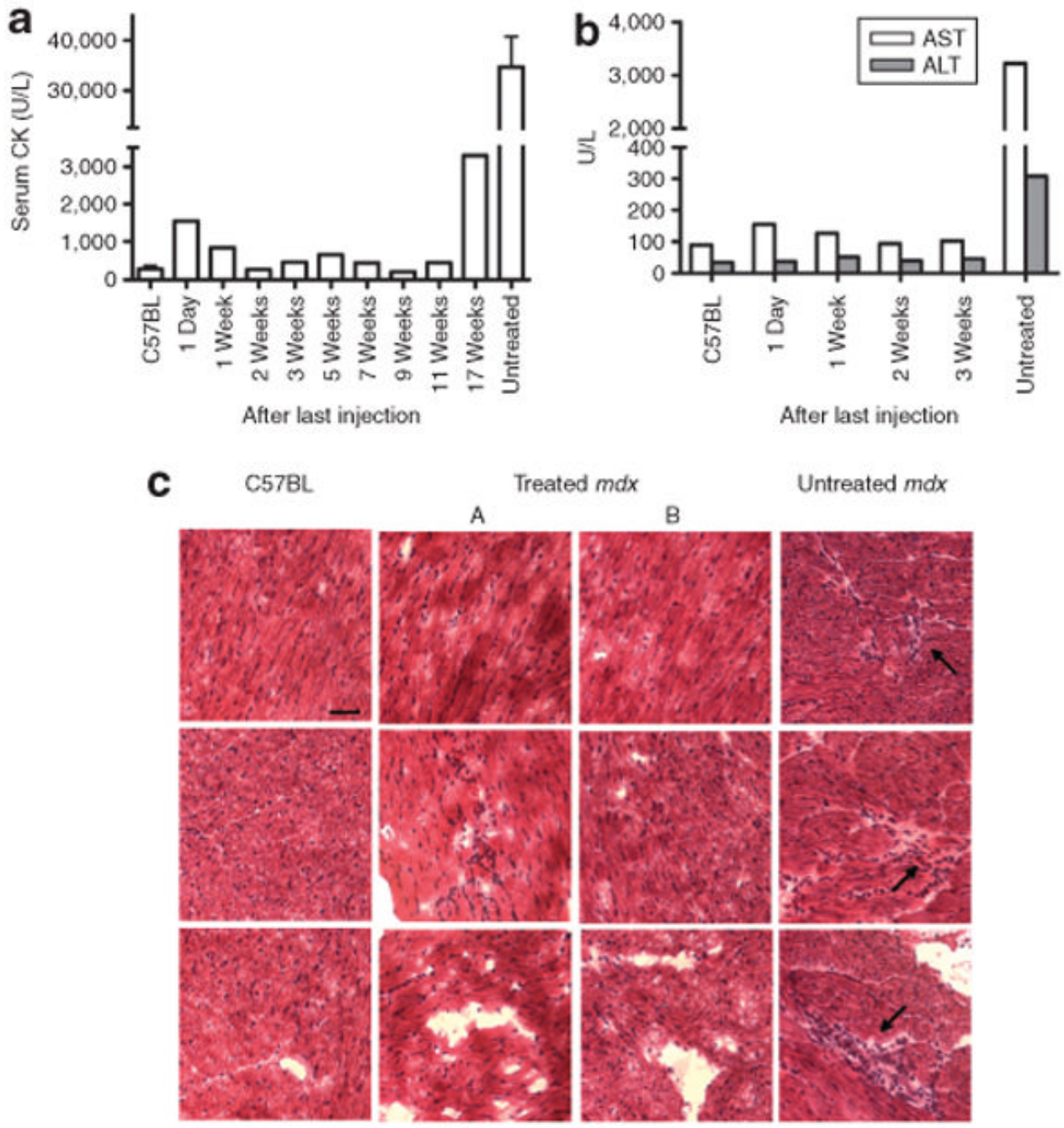

Figure 5. Improvement of pathology markers in *mdx* mice treated intravenously with M23D-B at 12 mg/kg/day for 4 days

(**a**) Serum creatinine kinase (CK). C57BL (n = 5), treated *mdx* mice (n = 2 at each time point), and untreated *mdx* mice (n = 20). (**b**) Serum aspartate aminotransferase (AST) and alanine aminotransferase (ALT). C57BL (n = 3), treated *mdx* mice (n = 2 at each time point), and untreated *mdx* mice (n = 10). All bar graphs represent mean except the bar graphs of serum CK of C57BL and untreated *mdx* mice, which represent mean and SEM. (**c**) Hematoxylin and eosin staining of cardiac muscle. C57BL at 8 weeks of age, treated *mdx* at 11 weeks of age (3 weeks after last injection), and untreated *mdx* at 8 weeks of age. Arrows, inflammatory infiltrate; Scale bar, 100 μm.

Table 1

Nomenclature and sequences of CPPs

Name	Sequence	Abbreviation	Length
A	RRRRRRRRXB	$(R)_8XB$	10
B	RXRRBRRXRRBRXB	$(RXRRBR)_2XB$	14
C	RXRRXRRXRRBRXB	$(RXR)_3RBRXB$	14
D	RBRBRBRBRBRXRBRXB	$(RB)_5RXRBRXB$	17
E	RBRBRBRXRBRBRBRXX	$(RB)_3RX(RB)_3RXX$	17
F	XRBRBRBRXRBRBRBRX	$X(RB)_3RX(RB)_3RX$	17
G	RBRXRBRXRBRXRBRXB	$(RBRX)_4B$	17
H	RBRBRBRBRXRXRXRXB	$(RB)_4(RX)_4B$	17
I	RXRBRBRXRBRBRBRXX	$RX(RB)_2RX(RB)_3RXX$	17
J	rXrrXrrXrrXrXB	$(rXr)_4XB$	14
K	RXRRXRRXRRXRXB	$(RXR)_4XB$	14
L	RBRBRBRBRBRBRBRBB	$(RB)_8B$	17
M	RBRBRBRBRBRBRBRXB	$(RB)_7RXB$	17
N	RBRBRBRBRBRBRBRBB	$(RB)_8B$	17

Abbreviation: CPP, cell-penetrating peptide.

B, β-alanine; r, D-arginine; R, L-arginine; X, 6-aminohexanoic acid.